

NUMERICAL AND EXPERIMENTAL MODELLING OF THREE PHASE DIRECT CONTACT HEAT EXCHANGERS

T. Coban and R. Boehm

Mechanical and Industrial Engineering Department
University of Utah, Salt Lake City, UT 84112 USA

A one-dimensional numerical model is developed for motion and heat transfer in a three-phase, spray-column, direct contact heat exchanger. General equations are defined for distance up the column using a physically-based model for the local heat transfer. A new formulation is given for a mixed, time-averaged temperature that may be representative of measurements taken with temperature transducers in direct contact heat exchangers. Results are compared to experimental data found from the operation of a 0.6 m dia, 6 m high spray column heat exchanger using pentane and water. Good agreement is shown between the predictions and the data.

ct Between continuous phase and thermocouple
d Dispersed phase
dt Between dispersed phase and thermocouple
l Liquid
mix Mixed value
o Initial
v Vapor

2. INTRODUCTION

Three-phase direct contact heat exchangers (DCHXs) have been proposed for a variety of applications including power generation and water desalination. A major thrust for the application of three-phase DCHXs for geothermal power generation has come from the US Department of Energy. This work recently culminated with the design, construction and operation of a 500 kW power plant at East Mesa, California. [1] A comprehensive summary of much of the early direct contact heat exchange work has been given. [2]

One of the major problems still present in this technical area is lack of comprehensive design tools. Since limited experiments have been performed, there is a lack of broadly applicable data. The few design techniques available today still require the use of empirical data. [2]

The key to a better understanding of these devices will almost certainly be through the development of numerical models that accurately reflect the heat transfer and fluid mechanics phenomena that are present. Little work has been successfully accomplished in this area. One of the more definitive efforts in this aspect has been directed toward the simulation of liquid/liquid spray columns, and this was presented by Jacobs and Golafshani. [3] They showed fair agreement between the results of their numerical model and the experimental results for the liquid/liquid portion of the East Mesa heat exchanger noted above. In another recent approach to this problem, a single droplet rising through a continuous phase has been modelled. [4] A single bubble analysis has been used quite frequently, and it is this type of approach that seems to offer a great deal of promise for the more complex spray column situation.

A number of studies have focussed one of the more critical aspects of the modelling: that of defining appropriate models for droplet heat transfer rates. One of the earliest workers in this area was Sideman, and he has performed both experiments and theoretical developments. [5,6] His theoretical approach is based upon a conduction-type solution in the semi-infinite (assumed) continuous fluid. Another group of early workers formulated an evaporation heat transfer model by considering conduction through the periodic sloshing layer of the dispersed phase liquid. [7]

More recently Raina and coworkers have dealt with several aspects of bubble behavior on a fundamental level. Included are the analysis of the instantaneous velocity [8] or general motion [9], a basic study of the heat transfer during change of phase [10] and a further analysis of heat transfer

1. NOMENCLATURE

A Bubble surface area
A_c Cross sectional area of the column
C Drag coefficient
D Diameter of droplet
D_o $(D^2 + D_o^2) / (2DD_o)$
g Acceleration due to gravity
h Heat transfer coefficient
h Combined heat transfer coefficient
h Enthalpy
i Counter index
k Thermal conductivity
k Correlation factor
m Mass flow rate
M Ratio of liquid density to vapor density
Nu Nusselt number
n Number of drops per unit volume
P Pressure
Pe Peclet number
Pr Prandtl number
Q Heat transfer rate
r Radial coordinate
R Outside radius of sphere or bubble
Re Reynolds number
t Time
T Temperature
U Velocity
V Volume
x Quality
z Vertical distance along column from bottom
 α Thermal diffusivity
 β Vapor half opening angle in bubble
 η Ratio: heat transfer to the bubble to heat transfer from the continuous phase
 γ Constant rate of increase of surface temperature with time
 ϕ Holdup ratio
 μ Viscosity
 ρ Density
Subscripts
ave Average value
c Continuous phase
cd Between continuous and dispersed phases

considering sloshing effects [11]. The basis of the Raina heat transfer mechanism is to consider heat transfer only through the liquid layer in the bottom of the droplet and to assume that, other than the area effects of the layer, the heat transfer resistance exists only in the continuous phase.

Several others have performed various experimental studies, where the objective was either the development of empirical correlations of heat transfer behavior, or the observation of microscopic behavior of the droplet. [12,13,14,15]

Physically the overall heat transfer coefficient for a liquid bubble rising in a continuous liquid phase should increase as the relative velocity of the bubble increases (assuming that the bubble is injected essentially from rest.) As evaporation begins inside the droplet, the overall heat transfer coefficient may continue to increase due to the enhanced heat transfer due to evaporation in the bubble and acceleration of the bubble; or could start to decrease due to a greater amount of low conductivity vapor contained in the droplet. At some point the latter characteristic must appear. Finally, the heat transfer coefficient should reach a low value associated with the completely vapor situation. Any changes from that point to the end of the heat transfer process should be minor, trading off the enhanced heat transfer associated with an increase in buoyancy related velocity against the poorer internal heat transfer characteristics of larger bubbles. More background information on the various forms of heat transfer coefficients is given in the description of the model development.

The work reported here is an attempt to develop a calculational procedure to describe the flow and heat transfer of droplets of one substance (the dispersed phase) through the bulk flow of a second fluid (the continuous phase). Gravity effects on the difference in densities of the two fluids are assumed to drive the flow. It is also desired to formulate the results so that they can be compared to typical experimental measurements. In all cases in what follows, any possible mass transfer effects are neglected.

3. MODEL DEVELOPMENT

3.1 General Aspects

The development of the governing equations for the numerical model start with the continuity equations. Using the assumption that the mass flow rates for both the continuous and dispersed phases remain constant, the continuity equations can be written as:

$$m_d = \rho_d (A \phi) U_d \quad (1)$$

$$m_c = \rho_c [A (1 - \phi)] U_c \quad (2)$$

where m_d , ρ_d , and U_d are the mass flow rate, density and velocity of the drop, which is also referred to as the dispersed phase. The same quantities with the c subscript refer to the continuous phase. A is the cross sectional area of the column and ϕ is the holdup ratio.

A momentum equation for the total flow can be written as:

$$\frac{d}{dz} [\rho_d U_d^2 \phi] + \frac{d}{dz} [\rho_c (1 - \phi) U_c^2] = -\frac{dP}{dz} - [\rho_c (1 - \phi) + \rho_d \phi] g \quad (3)$$

Substituting the continuity equations (1) and (2) into equation (3) and rearranging gives equation (4).

$$\frac{dP}{dz} = -\frac{m_d}{A} \frac{dU_d}{dz} - \frac{m_c}{A} \frac{dU_c}{dz} - [\rho_c (1 - \phi) + \rho_d \phi] g \quad (4)$$

This equation is used to determine the change of pressure along the column. Note that the third term on the right hand side of this equation reflects changes in the hydrostatic component of the pressure, while the first two terms on the right hand side represent the velocity effects on pressure.

The one dimensional energy equations for the dispersed and continuous phases in the column are given in terms of the enthalpy by the following:

$$\frac{d}{dz} [\rho_d \phi U_d h_d] = \frac{Q}{V} \quad (5)$$

$$\frac{d}{dz} [\rho_c (1 - \phi) U_c h_c] = -\frac{\eta Q}{V} \quad (6)$$

Here η is the ratio of the heat transfer from the continuous phase divided by the heat transfer to the dispersed phase. For situations where there is heat loss to the ambient, this ratio will be greater than unity. It is assumed that the heat loss originates from the continuous phase. Substituting equations (1) and (2) into equations (5) and (6) results in the following relationships.

$$\frac{d h_d}{dz} = \frac{A}{m_d} \frac{Q}{V} \quad (7)$$

$$\frac{d h_c}{dz} = -\frac{A}{m_c} \frac{\eta Q}{V} \quad (8)$$

A relationship for the velocity variation is found from a force balance equation. The difference between the dispersed and continuous phase velocities is given as:

$$U_d - U_c = \left[\frac{4 (\rho_c - \rho_d) D g}{3 \left(\frac{\rho_d}{\rho_c} \right) C} \right]^{1/2} \quad (9)$$

Raina and coworkers [8,9] used this equation with experimental data to find the following relationship.

$$U_d - U_c = \frac{\left[\frac{4 \left(\rho_d D_o^3 \right) D g}{3 \left(\frac{\rho_d}{\rho_c} \right) C} \right]^{1/2} D^{5/6 - D/T_c}}{\left[\frac{T_c^2 + T_d^2}{2 T_c T_d} \right]^{1/D} Pr_c^{D_o/1.6D}} \quad (10)$$

For calculating the drag coefficient an experimentally determined curvefit for a solid sphere is combined with a correlation for Stoke's drag force for the liquid droplet. [16] The resulting equation is given by:

$$C = \left[\frac{24}{Re} + \frac{6}{1 + Re^{1/2}} + 0.4 \right] \left[\frac{1 + 2 \mu_c / 3 \mu_d}{1 + \mu_c / \mu_d} \right] \quad (11)$$

This result was compared with several others in the literature and gave comparable results. In all cases the droplets were assumed to be spherical. See the discussion later about this assumption.

The expression for the bubble diameter was found by

assuming conservation of dispersed phase mass flow rate, and by further assuming that the bubbles did not break up or coalesce. An expression like equation (12) results.

$$D = D_o \left[\frac{\rho_c U_d}{\rho_{co} U_{do}} \right]^{1/3} \quad (12)$$

Coalescence can be easily added to this by including an empirical function for the attenuation of the number of bubbles with height, while maintaining the flow rates constant.

3.2 Heat Transfer Coefficient

A very critical area in the model is the representation of the heat transfer coefficient. While several models exist in the literature, as was noted above, there are problems with all of them. We briefly review below several of the ones mentioned above. First consider the evaporation region.

Sideman and Taitel [6] obtained the following equation.

$$Nu_c = \left[\frac{3 \cos \beta - \cos^3 \beta + 2}{\pi} \right]^{1/2} Pe_c^{1/2} \quad (13)$$

where β is the vapor half opening angle and can be calculated from the following expression.

$$(3 \cos \beta - \cos^3 \beta + 2) = \frac{4(1-x)}{1+x(M-1)} \quad (14)$$

In this equation, x is the quality and M is the ratio of liquid density to the vapor density. Later, Sideman and Isenberg [5] suggested a correction factor to this relationship given as

$$k = 0.25 Pr_c^{-1/3} \quad (15)$$

The modified form of the equation (13) is given in equation (16).

$$Nu_c = \left[\frac{3 \cos \beta - \cos^3 \beta + 2}{\pi} \right]^{1/2} (0.25 Pe_c Pr_c^{-1/3})^{1/2} \quad (16)$$

and Tochitani et al. [14] suggested that

$$Nu_c = Pe_c^{1/3} \{ 0.466 [\pi - \beta + (\sin 2\beta)/2]^{2/3} \} \quad (17)$$

In all of these equations, the term in the braces is the ratio of the surface area of liquid in the bubble compared to the total bubble area. In all cases, it is assumed that potential flow is present on the outside of the bubble. Also, all of the approaches indicated neglect any heat transfer through the vapor portion of the bubble. If this type of model is used, it is obvious that it would take an infinite distance for complete vaporization to occur. Since equation (17) represents only the resistance to heat transfer between the liquid in the bubble and the continuous phase, it will be denoted as an expression for Nu_{l1} to emphasize the liquid mode.

To allow a more realistic form of heat transfer to be modelled, obviously some vapor heat transfer mechanism must be incorporated. For small bubbles a conduction model may represent the energy flow in the vapor.

Carslaw and Jaeger [17] have tabulated the solution for the temperature response inside a sphere (initially at zero temperature) when the surface temperature is varied linearly with time (i.e. as γt). This type of boundary condition is somewhat like that encountered by a bubble rising into warmer and warmer fluid. The solution is:

$$T = \gamma \left[t - \frac{R^2 - r^2}{6\alpha} \right] - \frac{2\gamma R^3}{\alpha\pi^3 r} \sum_{i=1}^{\infty} \frac{(-1)^i}{i^3} e^{-\alpha i^2 \pi^2 t / R^2} \sin \frac{i\pi r}{R} \quad (18)$$

Now form the expression for the average temperature in the sphere from this equation. Taking simply the "steady" portion of the time variation, equation (19) results.

$$T_{ave} = \gamma (t - R^2 / 15\alpha) \quad (19)$$

Since γt is the surface temperature of the bubble, this equation can be used to find the temperature difference between the surface and the average in the bubble. This difference is independent of time explicitly, although it can vary implicitly through a variation of R with time. The heat transfer is found by using Fourier's law, yielding the following:

$$Q = k A \gamma R / (3\alpha) \quad (20)$$

Using the usual definition of the heat transfer coefficient, equations (19) and (20) give the following result.

$$h_v = 5 k_v / R \quad (21)$$

The combination of the liquid and the vapor components of the heat transfer can be written on an area weighted basis. This will be given as:

$$\bar{h} = h_l \frac{A_l}{A} + h_v \frac{A_v}{A} \quad (22)$$

Note that both liquid-based formulation of Sideman [5,6] and one of Tochitani [14] have incorporated this type of area ratio in them. For example, from the Tochitani formulation, the following is given:

$$\frac{A_l}{A} = 0.466 \left[\pi - \beta + \frac{\sin 2\beta}{2} \right]^{2/3} \quad (23)$$

Since the total area of the bubble must be in contact with either liquid or vapor:

$$A_v / A = 1 - A_l / A \quad (24)$$

Then the total heat transfer coefficient for evaporation portion of the column can be written as:

$$\bar{h} = Pe_c^{1/3} k_l \{ 0.466 [\pi - \beta + (\sin 2\beta)/2]^{2/3} \} / 2R + 5k_v \{ 1 - 0.466 [\pi - \beta + (\sin 2\beta)/2]^{2/3} \} / R \quad (25)$$

All that remains for a complete description is to define the techniques used in the liquid/liquid portion of the column. The important aspect here is the way the heat transfer coefficient internal to the drop was calculated. The result given by Sideman and Shabtai [18].

$$Nu_d = 0.00375 Pe_d / [1 + \mu_c / \mu_d] \quad (26)$$

The outside heat transfer coefficient is calculated as described earlier, and the inside and outside values are combined in series resistances to yield the overall resistance.

3.3 Combined Temperature Formulation

One final item is necessary. To be able to compare the results of any model that computes separate temperatures for both the continuous and the dispersed phases throughout the

column to experimental measurements, a special formulation is necessary. This is because any experimentally used temperature measuring device will necessarily sense some time-averaged value of the combined effects of the dispersed and continuous phases.

Consider a volume region in the column that is imagined to be the element monitored by the temperature measuring device. It is assumed that the statistical time average reading of the thermocouple is determined by the thermal transport to the thermocouple from the dispersed and continuous phases over some total (and arbitrary) amount of time. This time can be determined from the holdup ratio and each phase's velocity. Therefore the apparently mixed temperature reading will be:

$$T_{\text{mix}} = \frac{h_{dt} U_d \Delta t T_d + h_{ct} U_c \Delta t T_c}{h_{dt} U_d \Delta t + h_{ct} U_c \Delta t} \quad (27)$$

Here h_{dt} and h_{ct} are the heat transfer coefficients for the dispersed and continuous phases (respectively) to the thermocouple. Note that $U_d \Delta t$ and $U_c \Delta t$ are the total volumes covered simultaneously in the response time Δt . Assuming that there is the previously supposed one direction for the travel of the two phases (albeit opposite in sign), the total travel distance in the time Δt should be Δx_c and Δx_d . There the total volume each phase covered during this distance interval can be written as shown in the equations below without regard to sign.

$$U_d \Delta t = A_d \Delta x_d = A \phi \Delta x_d = A \phi U_d \Delta t \quad (28)$$

$$U_c \Delta t = A_c \Delta x_c = A (1-\phi) \Delta x_c = A (1-\phi) U_c \Delta t \quad (29)$$

By combining equations (28) and (29) with equation (27), the mixed temperature is found as shown in equation (30).

$$T_{\text{mix}} = \frac{h_{dt} \phi U_d T_d + h_{ct} (1-\phi) U_c T_c}{h_{dt} \phi U_d + h_{ct} (1-\phi) U_c} \quad (30)$$

Heat transfer coefficients for the thermocouple were calculated separately either for single phase or evaporation situations from correlation given in Kreith [19].

3.4 Computational Methods

In carrying out the numerical solutions, the governing differential equations are solved by using an Euler method. Because of the initial condition of the continuous phase is at the top of the column, but the computational scheme begins at the bottom of the column, a shooting method with a fourth degree curvefit is used to determine the complete set of initial conditions.

The computational order progresses in the following manner. First the velocity of the dispersed phase is calculated. Then the holdup ratio and the continuous phase velocity are found from the continuity equation. Then the droplet radius is found. Derivatives of the velocity terms are assumed to be zero initially, then the derivatives are calculated. The momentum and energy equations are solved for their derivatives. The functional values of pressure and enthalpies are calculated. In the boiling region the quality of the dispersed phase is calculated and the enthalpy is found as a function of quality and pressure. At each calculational level in the boiling region, the quality is also changed as function of the hydrostatic pressure. Stepwise quality corrections for the pressure change are calculated and added to the quality change due to heat transfer.

Due to the empirical form of the velocity profiles used, the

derivatives of the velocities are calculated from difference equations. The half opening angle, β , is solved by a Newton iteration technique. Transport properties were evaluated from published values.[20] Thermodynamic properties of pentane and water are calculated by the subroutines developed here.[21]

4. EXPERIMENTS

Experiments were performed in a 0.61 m diameter tower that measured 6.1 m tall and that was made entirely of conventional pipe. For the experiments that yielded the data to be cited later, the active level of continuous phase fluid (water) was kept at approximately 3.05 m. Water entered into the top of the column at 85°C flowed downward through the column and exited at the bottom. Commercial grade normal pentane was used as the dispersed phase fluid. The pentane entered the bottom of the column through a multiple showerhead arrangement, flowed upward in droplet form while vaporizing, and exited at the top of the column as vapor. Design of the showerhead was such that initial pentane droplet diameters of approximately 3-4 mm were produced. Operating pressures of approximately 2-3 atm were normally used in the column.

Orifice plates were used to measure the flowrates of the hot water and the liquid pentane. Pressure transducers were connected in parallel with manometers to indicate the pressure drops. Temperature measurement was accomplished with the use of shielded Chromel-Alumel thermocouples. 24 were used to determine temperature throughout the system, including the inlet and outlet stream temperatures as well as bulk temperatures at various locations within the column.

External heat exchange function were accomplished by three devices. On the water side, a plate heat exchanger was used. Steam at approximately 6 atm and 150°C was used to heat the water. To condense the pentane, two shell-and-tube heat exchangers were used. One of these two devices served essentially as a desuperheater and the other served as a condenser. Ambient temperature water was used for condensing the pentane.

Both the pentane and water loops to the DCHX were completely closed other than in the column where they came in contact. Water and pentane liquid were both stored in 1900 liter tanks during operation. Pumping was accomplished by centrifugal, explosion-proof, stainless steel pumps. Bypass lines around the pumps were used for control.

Data analysis took place after each day's operation. The analysis technique involved simple energy balances on each of the fluids as well as on the column as a whole. Both calibrations and calculated estimates of heat loss from the vessel were used in predicting the net heat transfer between the fluids.

Further information about the experiments can be found in a previous paper. [22]

5. RESULTS AND DISCUSSION

Temperature profiles for the same experimental and numerical model boundary condition have been investigated. One of the resultant curve set which represents the maximum dispersed phase mass flow rate is given in Figure 1. Experimentally measured temperatures are shown and should be compared to the "mixed" temperature distribution. In these calculations mass flow rate of the pentane is assumed to be 0.12 kg/sec and the mass flow rate of water is taken as 1.91 kg/sec. These conditions compare exactly to the experimental data shown in Figure 1. (Note that at each end of the column there are a pair of experimentally measured temperatures shown. These represent the temperatures of both of the streams exiting and entering at that end of the column.) Good agreement is shown between the measured and calculated values. The exiting and entering temperatures are very closely approximated, and the mixed temperature variation is qualitatively similar.

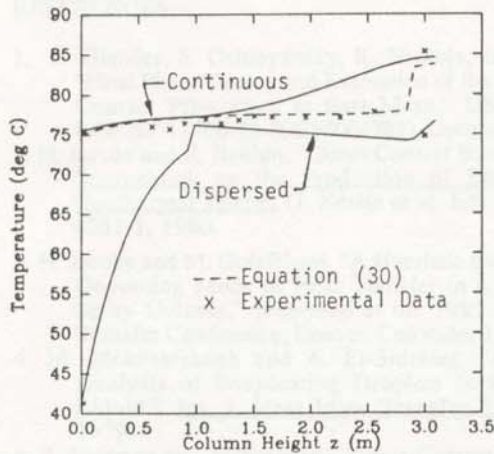


Figure 1. A plot of calculated (solid lines) temperatures and one set of measurements for similar conditions from an experiment. The "mixed" temperature should be compared to the experimental values. There are two values of experimental temperatures shown at each end, representing the four flow streams in and out.

Contrary to intuition, a fairly flat temperature profile in a spray column does not necessarily imply large amounts of backmixing, premature boiling or a number of other oft-cited possible shortcomings of spray columns. The present hypothesis yields results that are nearly the same as the experimentally determined values and could be quite close to the actual situation.

Even though some of the previously developed heat transfer correlations yielded good results here, there was a need to propose a correlation for the superheated vapor phase. Equation (21) seems to represent this region very well.

The assumption of spherical bubbles was checked after the calculations were made. Comparisons to the plot given by Grace [23] indicated that most cases examined here resulted in spherical drops, and that only a few situations were slightly into the ellipsoidal region. Hence the spherical assumption may not be too far from the real situation for experiments described here.

In Figure 2 a number of existing correlations are compared. It is seen that they are not in good agreement. The two models of Sideman and coworkers [5,6] predict quite high values of heat transfer. In fact the values predicted are considerably higher than some of the more recently proposed correlations, one of which is the curve indicated as Tochitani [14]. This equation represents a large portion of the vaporization process more accurately, but it, like the Sideman predictions, does not allow a realistic amount of heat transfer through the vapor portion of the bubble. The model used in the present analysis is quite similar to the Tochitani prediction over much of the range of variables. However, the present correlation does account for energy transfer through the vapor portion of the bubble. In Figure 2, the Tochitani and the present predictions do overlap considerably. While the present work has focussed on a pentane-water system, more investigation is needed to compare it to other combinations of fluids.

A third figure (Figure 3) shows the variation of calculated values of quality and holdup ratio throughout the column. Although the bubble size becomes quite large near the later portions of the vaporization process, the bubble spacing widens, causing the holdup to remain moderate. Not included in the model is any representation of wake effects, droplet coalescence or droplet breakup. Effects of some of these elements will be incorporated in further developments of the model.

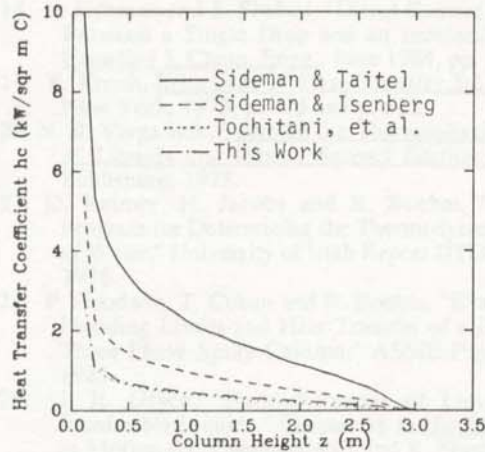


Figure 2. A comparison of four models to predict the overall heat transfer coefficient during vaporization: [5,6,14] and the correlation developed here. The latter corresponds closely to the Tochitani result except at high qualities.

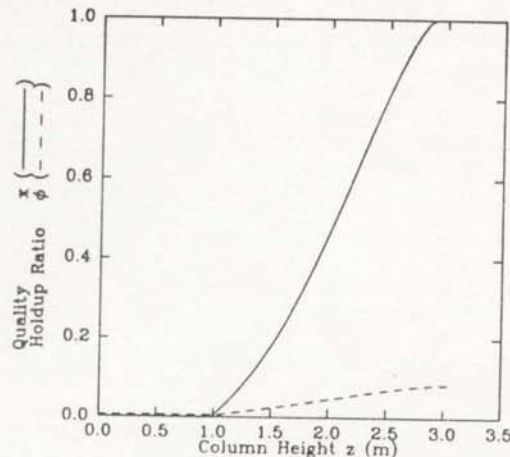


Figure 3. The calculated variation of quality and holdup ratio throughout the column for the situation shown in Figure 1.

6. CONCLUSIONS

A one-dimensional model of a three-phase spray column has been developed by considering the total flow inside the column along with the microphenomena that influence the motion and heat transfer to dispersed phase droplets. Existing heat transfer models have been modified to represent the physical situation more accurately. A mixed temperature quantity has been proposed as a simulation of the temperature that a thermocouple mounted in the column may indicate. The model appears to describe many of the general characteristics of the water-pentane spray column which was used in experiment. Checking the model with different continuous and dispersed phase fluids is needed to ensure its accuracy for a range of situations.

ACKNOWLEDGEMENT

The partial support of this work by the Solar Energy Research Institute and Utah Power and Light Company is gratefully noted.

REFERENCES

1. R. Olander, S. Oshmyansky, K. Nichols, and D. Werner, "Final Phase Testing and Evaluation of the 500 kW Direct Contact Pilot Plant at East Mesa," US DOE Report DOE/SF/11700-T1 (DE84004781), December 1983.
2. H. Jacobs and R. Boehm, "Direct Contact Binary Cycles," in Sourcebook on the Production of Electricity from Geothermal Energy (J. Kestin et al. Eds.), DOE/RAW/4051-1, 1980.
3. H. Jacobs and M. Golafshani, "A Hueristic Evaluation of the Governing Mode of Heat Transfer in a Liquid-Liquid Spray Column," presented at the 1985 National Heat Transfer Conference, Denver, Colorado, 1985.
4. M. Mokhtarzadeh and A. El-Shirbini, "A Theoretical Analysis of Evaporating Droplets in an Immiscible Liquid," Int. J. Heat Mass Transfer, **22**, pp. 27-38, 1979.
5. S. Sideman and J. Isenberg, "Direct Contact Heat Transfer with Change of phase: Bubble Growth in Three-Phase Systems," Desalination, **2**, pp. 207-214, 1967.
6. S. Sideman and Y. Taitel, "Direct Contact Heat Transfer with Change of Phase: Evaporation of Drops in an Immiscible Liquid Medium," Int. J. Heat Mass Transfer, **7**, pp. 1273-1289, 1964.
7. H. C. Simpson, G. Beggs and M. Nazir, "Evaporation of Butane Drops in Brine," Desalination, **15**, pp. 11-23, 1974.
8. G. K. Raina and R. Wanchoo, "Direct Contact Heat Transfer with Phase Change: Theoretical Expression for Instantaneous Velocity of a Two-Phase Bubble," Int. Comm. Heat Mass Transfer, **11**, pp. 227-237, 1984.
9. G. K. Raina, R. Wanchoo and P. Grover, "Direct Contact Heat Transfer with Phase Change: Motion of Evaporating Droplets," AIChE Journal, **30**, pp. 835-837, 1984.
10. G. K. Raina and P. D. Grover, "Direct Contact Heat Transfer with Change of Phase: Theoretical Model," AIChE Journal, **28**, pp. 515-517, 1982.
11. G. K. Raina and P. D. Grover, "Direct Contact Heat Transfer with Change of Phase: Theoretical Model Incorporating Sloshing Effects," AIChE Journal, **31**, pp. 507-510, 1985.
12. C. B. Parakash and K. L. Pinder, "Direct Contact Heat Transfer between Two Immiscible Liquids During Vaporization, Part I Measurement of Heat Transfer Coefficient," The Canadian Journal of Chemical Engineering, **45**, pp. 210-214 and "Direct Contact Heat Transfer between Two Immiscible Liquids During Vaporization, Part II, Total Evaporation Time," The Canadian Journal of Chemical Engineering, **45**, pp. 215-220.
13. A. Adams and K. Pinder, "Average Heat Transfer Coefficient during the Direct Evaporation of a Liquid Drop," The Canadian Journal of Chemical Engineering, **50**, pp. 707-713, 1972.
14. Y. Tochitani, Y. Mori and K. Komotori, "Vaporization of a Liquid Injected into an Immiscible Liquid through a Single Nozzle," Warme- und Stoffubertragung, **8**, pp. 249-259, 1975.
15. Y. Mori, and K. Komotori, "Boiling Modes of Volatile Liquid Drops in an Immiscible Liquid Depending on Degree of Superheat," presented at the 1976 National Heat Transfer Conference, 1976.
16. F. White, Viscous Fluid Flow, McGraw-Hill, 1974.
17. H. Carslaw and J. Jaeger, Conduction of Heat in Solids, Oxford, 1959.
18. S. Sideman and S. Shabtai, "Direct Contact Heat Transfer Between a Single Drop and an Immiscible Medium," Canadian J. Chem. Eng., June 1964, pp. 107-117.
19. F. Kreith, Principles of Heat Transfer, 3rd Edition, IEP, New York, 1973, p. 473 and p. 522.
20. N. B. Vargaftick, Table on the Thermophysical Properties of Liquids and Gases, Second Edition, Hemisphere Publishing, 1975.
21. D. Reimer, H. Jacobs and R. Boehm, "A Computer Program for Determining the Thermodynamic Properties of Water," University of Utah Report UTEC ME-76-171, 1976.
22. P. Goodwin, T. Coban and R. Boehm, "Evaluation of the Flooding Limits and Heat Transfer of a Direct Contact Three Phase Spray Column," ASME Paper 85-HT-49, 1985.
23. J. R. Grace, "Hydrodynamics of Liquid Drops in Immiscible Liquids," Chapter 38 in Handbook of Fluids in Motion (N. Chermisinoff and R. Gupta, Eds.), Ann Arbor Science, p. 1008.